Recruitment of Novel Calcium-Binding Proteins for Root Nodule Symbiosis in *Medicago truncatula*[1][W][OA]

Junqi Liu[2], Susan S. Miller[2], Michelle Graham[2,3], Bruna Bucciarelli, Christina M. Catalano, D. Janine Sherrier, Deborah A. Samac, Sergey Ivashuta, Maria Fedorova[4], Peter Matsumoto, J. Stephen Gantt, and Carroll P. Vance*

Department of Agronomy and Plant Genetics (J.L., M.F., P.M.) and Department of Plant Biology (M.G., S.I., J.S.G.), University of Minnesota, St. Paul, Minnesota 55108; United States Department of Agriculture, Agricultural Research Service, St. Paul, Minnesota 55108 (S.S.M., B.B., D.A.S., C.P.V.); and Department of Plant and Soil Sciences, Delaware Biotechnology Institute, University of Delaware, Newark, Delaware 19711 (C.M.C., D.J.S.)

Legume rhizobia symbiotic nitrogen (N_2) fixation plays a critical role in sustainable nitrogen management in agriculture and in the Earth's nitrogen cycle. Signaling between rhizobia and legumes initiates development of a unique plant organ, the root nodule, where bacteria undergo endocytosis and become surrounded by a plant membrane to form a symbiosome. Between this membrane and the encased bacteria exists a matrix-filled space (the symbiosome space) that is thought to contain a mixture of plant- and bacteria-derived proteins. Maintenance of the symbiosis state requires continuous communication between the plant and bacterial partners. Here, we show in the model legume *Medicago truncatula* that a novel family of six calmodulin-like proteins (CaMLs), expressed specifically in root nodules, are localized within the symbiosome space. All six nodule-specific *CaML* genes are clustered in the *M. truncatula* genome, along with two other nodule-specific genes, *nodulin-22* and *nodulin-25*. Sequence comparisons and phylogenetic analysis suggest that an unequal recombination event occurred between *nodulin-25* and a nearby calmodulin, which gave rise to the first *CaML*, and the gene family evolved by tandem duplication and divergence. The data provide striking evidence for the recruitment of a ubiquitous Ca^{2+}-binding gene for symbiotic purposes.

Plant acquisition of the macronutrient nitrogen in sustainable agricultural systems is dependent upon the symbiotic interaction between members of the plant family Fabaceae and the nitrogen-fixing soil bacteria in the family Rhizobiaceae (Mylona et al., 1995; Graham and Vance, 2003). This symbiotic process results in the de novo formation of a unique organ, the N_2-fixing root nodule. Root nodules arise from the coordinated expression of both rhizobial and plant genes in response to signals exchanged between the partners. Release of flavonoids/isoflavonoids from developing roots induce the expression of rhizobial nodulation genes and the synthesis of lipochitooligosaccharides. Lipochitooligosaccharides then activate the expression of a cascade of plant genes required for root nodule formation (Mylona et al., 1995; Geurts and Bisseling, 2002).

The completely developed root nodule contains both uninfected and infected cells (Vance, 2002). Within infected cells, rhizobia undergo endocytosis and become completely enclosed within a plant-derived membrane, creating in essence a new organelle, the symbiosome (Sym). The Sym space (SymS) is the matrix surrounding the bacterium (now termed bacteroid). Although the composition of this matrix and the role it plays in symbiosis is not well understood, it is known that an intact Sym membrane appears to be required for effective N_2 fixation and the exchange of low-M_r nutrients between the host plant and rhizobia (Udvardi and Day, 1997). Early studies identified the presence of protease, α-glucosidase, and α-mannosidase activities in the SymS (Mellor and Werner, 1987; Werner et al., 1988), but the possible relationship of these activities to symbiosis was not discerned. More recently, proteomic analysis of the Sym membrane from several legumes has identified numerous transport proteins, H^+-ATPases, chaperonins, a syntaxin, and both anion and cation

[1] This work was supported by the National Science Foundation Plant Genome Research Program award on *Medicago truncatula* genomics (DBI no. 0110206), the U.S. Department of Agriculture-Agricultural Research Service (CRIS project no. 3640–2100001900D to C.P.V.), and the National Research Initiative (CSREES grant nos. 2001–35318–10915 and 2001–35311–10161 to D.J.S.).

[2] These authors contributed equally to the paper.

[3] Present address: USDA-ARS CICGR Unit, Ames, IA 50011.

[4] Present address: DuPont Agriculture and Nutrition, Johnston, IA 50131.

* Corresponding author; e-mail vance004@umn.edu; fax 651–649–5058.

The author responsible for distribution of materials integral to the findings presented in this article in accordance with the policy described in the Instructions for Authors (www.plantphysiol.org) is: Carroll P. Vance (vance004@umn.edu).

[W] The online version of this article contains Web-only data.

[OA] Open Access articles can be viewed online without a subscription.

Article, publication date, and citation information can be found at www.plantphysiol.org/cgi/doi/10.1104/pp.106.076711.

channel proteins (Panter et al., 2000; Saalbach et al., 2002; Weinkoop and Saalbach, 2003; Catalano et al., 2004). Initial analysis of putative pea (*Pisum sativum*) SymS proteins revealed that bacteroid nitrogenase proteins were a major component of the SymS, but Saalbach et al. (2002) also detected five putative plant proteins. The occurrence of both intrinsic bacteroid and plant cytoplasmic protein in the SymS fraction suggests cross contamination may have occurred during isolation. Immunolocalization studies in pea suggest that a lectin-like protein and a Cys protease may be present in the Syms (Dahiya et al., 1997; Vincent and Brewin, 2000). The presence of a nodule-specific plant nuclear-encoded protein within the SymS has not been shown.

In a previous study, we identified six *Medicago truncatula* contigs that encode nodule-specific calmodulin-like (CaML) proteins (Fedorova et al., 2002). All the expressed sequence tag (EST) clones comprising the CaML contigs are derived from nodule or rhizobia-inoculated root cDNA libraries (GenBank AF494212–AF494216, AF494218). RNA blots demonstrated that the *M. truncatula* CaMLs are expressed only in root nodules. These CaML proteins were strikingly different from typical CaML proteins in that they contained a 30-amino acid presequence and a variable number of elongation factor (EF) hands. Computational analysis of the CaML presequences indicated that these proteins were targeted outside the cell. The nodule-specific nodulin-25 protein contains a presequence highly similar to the presequence in the *M. truncatula* CaML protein, and nodulin-25 was proposed to be in the SymS (Kiss et al., 1990). The occurrence of calcium-binding proteins in the SymS could potentiate a signal transduction process between the bacteroids and the host plant.

Calcium (Ca^{2+}) is a secondary messenger during signal transduction for a wide variety of stimuli in all eukaryotes (Sanders et al., 1999). Although cytoplasmic [Ca^{2+}] is usually in the nanomolar range (100–200 nM), biotic and abiotic stimuli induce transient increases in [Ca^{2+}], which act as a signal for cellular responses (Zielinski, 1998; White, 2000; Reddy, 2001; Snedden and Fromm, 2001). Calcium signals are transduced into cellular responses via Ca^{2+}-binding proteins, of which calmodulin (CaM) is the most common (Zielinski, 1998).

Changes in intracellular Ca^{2+} and signaling via Ca^{2+} are well-documented features of legume-rhizobia interactions and root nodule development (Lévy et al., 2004). Initial signaling of rhizobia bacteria to the legume root triggers two Ca^{2+} events, a rapid influx of Ca^{2+} into root hairs and transient Ca^{2+} spiking (Shaw and Long, 2003). Cytoskeletal remodeling, known to be regulated by Ca^{2+}-CaM, occurs within the root hair shortly following Ca^{2+} spiking (Shaw and Long, 2003). Recently, an *M. truncatula* gene (*DMI3*) with high sequence similarity to a Ca^{2+} and CaM-dependent protein kinase was shown to be integrally involved in the early events of both rhizobial and mycorrhizal symbioses (Lévy et al., 2004; Mitra et al., 2004). Whereas the role of Ca^{2+} in fully developed nodules is less clear, Krylova et al. (2002) reported a verapamil-sensitive Ca^{2+} transporter in the Sym membrane and Ca^{2+} accumulation in the SymS of *Vicia faba*. They also demonstrated that Ca^{2+} depletion of the Sym substantially decreased nitrogenase activity. Calcium also modulates malate uptake by Syms and a voltage-dependent cation efflux channel in the Sym membrane (Udvardi and Day, 1997; Roberts and Tyerman, 2002). Moreover, typical CaM mRNA and protein are found in Phaseolus, Glycine, Lotus, and *M. truncatula* root nodules (Webb et al., 2000; Camas et al., 2002; Fedorova et al., 2002). Based upon RNA expression and in situ hybridization patterns, Son et al. (2003) recently proposed that the divergent soybean (*Glycine max*) *SCaM-4*, detected in the infection zone of forming nodules (containing 32 amino acid substitutions from the highly conserved soybean CaM with no presequence apparent), may be required for endocytosis of Bradyrhizobium in soybean nodules.

Herein we tested the hypothesis that *M. truncatula* CaMLs are located in the Sym and the genes are clustered in the Medicago genome. We show that a *M. truncatula CaML1* promoter:reporter gene fusion is expressed in infected cells, a *CaML*:green fluorescent protein (GFP) translational gene fusion is expressed in the SymS, CaML proteins are localized within SymS, and an ancestral *CaM* gene appears to have been coopted for symbiotic purposes.

RESULTS AND DISCUSSION

CaML Expression in *M. truncatula* Root Nodules

Our earlier in silico analysis of the *M. truncatula* EST gene index (The Institute for Genomic Research [TIGR] MtGI at www.tigr.org/tdb/mtgi) indicated *CaML1* to *6* expression to be specific in root nodules (Fedorova et al., 2002). To determine developmental onset and confirm root nodule specificity of expression, a labeled DNA probe corresponding to *CaML1* was hybridized to total RNA samples from developing nodules (8, 10, and 14 d after inoculation [DAI]) and various tissues (Fig. 1A). *CaML1* transcripts were detected only in the 8-, 10-, and 14-DAI nodule RNA samples. To assess whether all *CaML* transcripts were expressed synchronously and whether they could be detected even earlier than 8 DAI, quantitative reverse transcription (RT)-PCR using gene-specific primers for all six CaML genes was carried out on total RNA purified from uninoculated root tissue (0 DAI), inoculated roots (3 DAI), root segments containing small nodules at 6 and 8 DAI, and nodules at 10 DAI (Fig. 1B). *CaML* mRNA was initially detected at 6 DAI, followed by a substantial increase in mRNA abundance between 6 and 8 DAI for all *M. truncatula* nodule-specific *CaML*s. A typical *CaM* gene (*CaM1*), also analyzed by RT-PCR as an internal control, showed constitutive expression. Taken together, the RNA blot and RT-PCR analysis indicated that expression of all members of the *CaML*

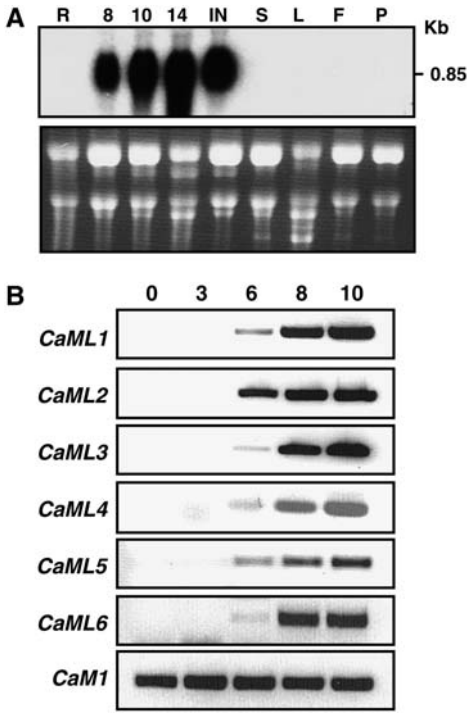

Figure 1. Analysis of *CaML1* expression in *M. truncatula*. A, RNA gel-blot analysis in developing nodules and in various tissues. Each lane in the top image contains 15 μg of total RNA from root (R), effective nodules 8 DAI (8), 10 DAI (10), and 14 DAI (14), ineffective nodules induced by *S. meliloti* strain T202 (IN), stem (S), leaf (L), flower (F), and pod (P). The blot was hybridized with a cDNA insert specific for the *CaML1* transcript. The numbers at the right indicate the size of the hybridizing band in kilobases. The bottom image shows the ethidium bromide-stained rRNA on the gel prior to blotting to the membrane. B, Semiquantitative RT-PCR analysis of *CaMLs* during nodule initiation. Total RNA was isolated from uninoculated roots (0), inoculated roots at 4 DAI (4), root segments with nodules at 6 and 8 DAI (6, 8), and nodules 10 DAI (10) and used for RT and subsequent PCR to detect transcript accumulation. Typical CaM transcript (*CaM1*) was also amplified as a positive control. Thirty cycles were used for the amplification of CaM1 and 26 to 36 cycles for CaML1 to 6.

gene family in *M. truncatula* is synchronous with nodule development and the onset of N_2 fixation (i.e. from 7–8 DAI).

We localized *CaML1* transcripts in *M. truncatula* nodules via in situ hybridization. Nodule nomenclature is classified according to Vasse et al. (1990): meristem (I), invasion zone (II), interzone (*), nitrogen-fixing zone (III), and senescent zone (IV). All infected cells within the nodule show a strong signal, with the highest expression of transcripts in cells of the early N_2-fixing zone (III; Fig. 2, A and B). The transcript was not detected in uninfected cells (Fig. 2B). Hybridization with a 3′-specific probe gave similar results (data not shown). In contrast, the constitutive *CaM1* (GenBank AF494219) transcript was uniformly distributed in all cells throughout the nodule, whereas tissue labeled with the control sense transcripts of *CaML1* showed no detectable signal above background (data not shown).

Ineffective nodules induced by *Sinorhizobium meliloti* strain T202, a mutant that causes early nodule senescence, accumulate *CaML1* transcripts in two to three cell layers of the late interzone (*) and early N_2-fixing zone (III; Vasse et al., 1990; Figs. 1A and 2C). These are the only cells in T202-induced nodules that contain bacteroids. *Leghemoglobin* transcripts accumulated in comparable nodule sections with a pattern similar to the *CaML1* transcripts (data not shown).

Nitrogen fixation can be observed in *M. truncatula* nodules as early as 7 to 8 DAI as measured by acetylene reduction activity (S.S. Miller and C.P. Vance, unpublished data). We were able to confirm that all *CaML* transcripts were present in nodule tissue at 6 DAI by RT-PCR. CaML1 β-glucuronidase (GUS) reporter gene activity was observed at 6 DAI using root segments containing small, but visible nodules as starting material. Whereas the RT-PCR technique is a highly sensitive method for transcript detection, acetylene reduction is known to be a less rigorous measure of the ability of plants to fix nitrogen. It was therefore not unexpected that the CaML transcripts can be detected before appreciable ethylene can be measured via gas chromatography. Mitra and Long (2004) noted a similar pattern of expression for CaML1 in effective nodules and in ineffective nodules containing limited bacteroid development. In addition, we detected *CaML1* transcripts in the late interzone of effective and ineffective nodules. Within this zone, rhizobia enlarge and nitrogenase becomes active as the bacteria develop into bacteroids within Syms. The presence of CAML1 transcripts at the outset of bacteroid development within the infected cells implies an early role for Ca^{2+} signaling in this crucial developmental process and continued maintenance of the bacteroid state.

We transformed alfalfa (*Medicago sativa*) with a chimeric *CaML1* promoter:GUS transcriptional fusion to determine nodule cell-specific expression. In addition, we constructed a *CaML1*:GFP translational fusion driven by the native *CaML1* promoter to analyze the subcellular location of CaML1 protein. Only the infected cells in the N_2-fixing zone of effective nodules showed GUS activity (Fig. 2D). Substantial GUS staining was also detected in very young nodules at the time of differentiation of bacteroids (6 DAI; data not shown). In agreement with GUS results, GFP-specific fluorescence was detected only in infected cells of the N_2-fixing zone of young nodules (Fig. 2, E–G). Infected cells were distinguished from uninfected cells by the intense staining of the bacterial nucleic acids by SYTO63 stain. High magnification of infected cells shows the GFP associated primarily with rod-shaped Syms within infected cells (Fig. 2H). When Syms were gently released from infected cells into the osmoticum, GFP was associated exclusively with the released Syms and not detected in the cytosol or other released cell contents (Fig. 2I).

Immunolocalization studies were done to further resolve the subcellular localization of CaML1 protein in root nodule-infected cells (14 DAI; Fig. 2, J–M).

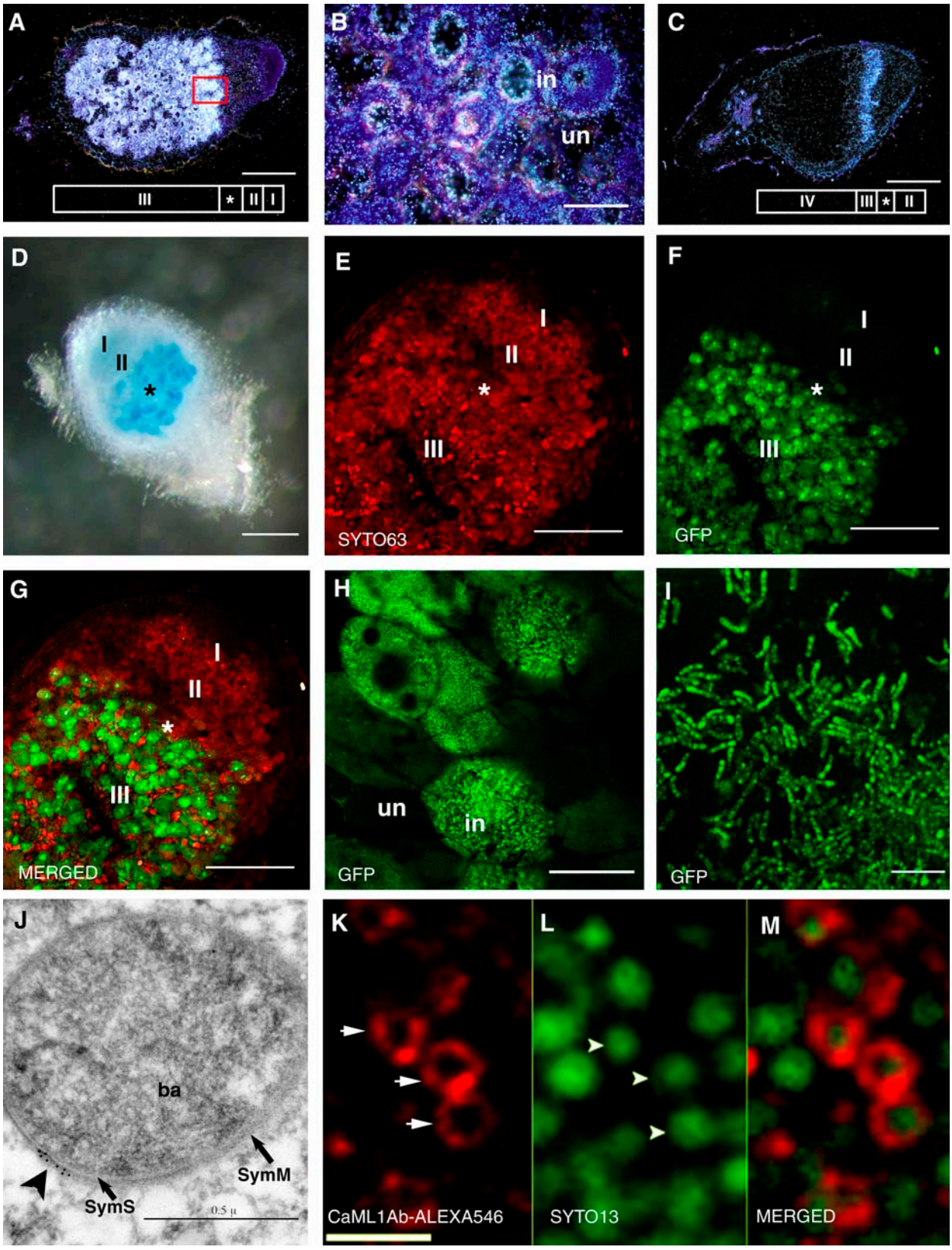

Figure 2. Localization of CaML1 transcripts and protein within Medicago root nodules. Nodule nomenclature is classified according to Vasse et al. (1990): meristem (I), invasion zone (II), interzone (*), nitrogen-fixing zone (III), and senescent zone (IV). Un, Uninfected cell; in, infected cell; ba, bacteroid; SymM, symbiosome membrane. A to C, Longitudinal cross section of mature

Immunogold localization studies showed CaML1 labeling in the SymS (Fig. 2J, arrowhead). Control sections in which CaML1 protein was used as a blocking agent resulted in no labeling of the SymS (data not shown). Laser-scanning confocal microscopy of nodule cells stained with affinity-purified CaML1-specific antibodies showed the anti-CaML1 signal is only present in infected cells. The CaML1 signal localized to areas surrounding and in contact with bacteroids: These areas correspond to the location of the SymS (Fig. 2, K–M). No antibody-reactive material was detected in the cytosol. These data, taken together with the structural and functional genomics as well as the biochemical data, indicate that CaML1 protein localizes to the SymS.

Additional evidence that CaML1 antibodies recognized CaML protein in nodules and the SymS was obtained by first identifying CaML cross-reactive proteins on western blots and then sequencing the immunoreactive protein. SymS proteins were isolated by differential centrifugation and the purity was assessed on a western blot using antibodies against leghemoglobin and phospho*enol*pyruvate carboxylase, abundant proteins of the nodule cytosol. Neither polypeptide was recognized. Catalano et al. (2004) have further tested this SymS fraction and found it to be devoid of nodulin-26, a Sym membrane protein. CaML1 antibody reacted strongly with the recombinant His-CaML1 protein at 17 kD (Fig. 3A, lane 6) and with comparable-sized bands in SymS protein (14 DAI, lane 5) as well as both 10 and 14 DAI total nodule protein (lanes 3 and 4). No immunoreactive polypeptides were detected in either root total protein (lane 1), nodule protein corresponding to 8 DAI (lane 2), or in leaf, stem, cotyledon, flower, or pod total protein (data not shown).

Tandem mass spectrometry (MS) following trypsin digest was used to further characterize the CaML immunoreactive polypeptides detected upon SDS-PAGE separation of SymS proteins. Search of the translated National Center for Biotechnology Information nonredundant database yielded matches corresponding to two *M. truncatula* nodule CaML proteins. One match corresponded to a unique 11-amino acid peptide (amino acids 142–152) from the CaML2 protein and the other match corresponded to a unique 11-amino acid peptide (amino acids 104–114) from the CaML5 protein.

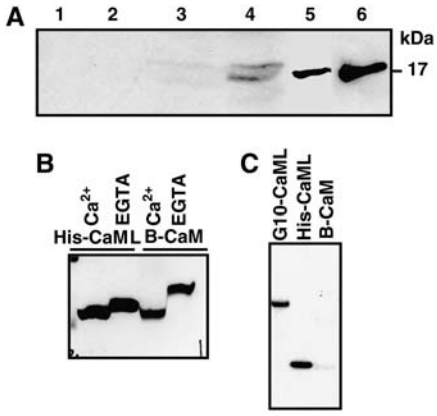

Figure 3. CaML protein is abundant in the SymS. A, Immunoblot detection of CaML protein using specific antibodies on cell-free extracts from roots (lane1), nodules 8 DAI (lane 2), 10 DAI (lane 3), and 14 DAI (lane 4), purified SymS protein (lane 5, 40 μg), and His-CaML protein (lane 6, 90 ng). Lanes 1 through 4 each contained 100 μg protein. The numbers at the right of each image indicate M_r markers in kilodaltons. B, Electrophoretic mobility shift assays on minigels in the presence (Ca^{2+}) or absence (EGTA) of calcium carried out on His-CaML protein (His-CaML) and on a typical bovine CaM (B-CaM) as a control. C, Analysis of the ability of the purified fusion proteins G10-CaML protein (G10-CAML) and His-CaML protein and a typical bovine CaM to bind ^{45}Ca on a nitrocellulose miniblot after SDS-PAGE.

It is estimated that as many as 200 proteins exist at the interface of the bacteroid and plant cell in *M. truncatula* (Catalano et al., 2004) and Pisum (Saalbach et al., 2002) nodules. Since the SymS does not contain its own protein translation machinery, essential proteins must be imported (Simonsen and Rosendahl, 2002). Catalano et al. (2004) proposed that proteins may be targeted to the SymS by the translation on free cytosolic ribosomes followed by protein insertion in the Sym membrane via N-terminal sequence recognition. Kiss et al. (1990) showed that alfalfa nodulin-25 protein has an N-terminal extension with a predicted 24-amino acid presequence. Catalano et al. (2004) identified *M. truncatula* nodulin-25

Figure 2. (*Continued.*)
effective and ineffective *M. truncatula* root nodules hybridized with antisense CaML1 probe. High expression of *CaML1* is found in the infected cells throughout effective *M. truncatula* root nodules in A and B. B, Magnification of the boxed area in A. Mature ineffective root nodules induced by *S. meliloti* strain T202 can be seen in C. Note *CaML1* transcripts are detected only in infected cells of the late interzone (*) and early zone III of ineffective nodules. Scale bars in A and C are 0.5 mm; in B, 0.02 mm. D, CaML1:GUS reporter gene activity in effective alfalfa nodules at 8 DAI (scale bar = 0.3 mm). E to I, Confocal images of CaML1:GFP localization in effective alfalfa nodules. Nodules stained with SYTO63 (E) nucleic acid stain showing location of nucleic acids in red. GFP localization in nodule in E visualized by scanning with 488-nm laser line (F). Overlay of E and F resulted in G, showing GFP is exclusively localized in infected cells. Scale bars in E to G are 0.25 mm. Magnification (60 ×) of cells in zone III (H) shows GFP reporter gene activity localized in Syms of infected cells (scale bar = 0.02 mm). CaML1:GFP reporter gene activity (I) is localized in Syms released from infected cells (scale bar = 0.01 mm). J, Immunogold localization of CaML1 protein in alfalfa root nodules. Arrowhead points to gold particles (scale bar = 0.5 μm). K to M, Immunolocalization of CaML1 in *M. truncatula* root nodule Syms using CaML1 primary antibodies and secondary antibody conjugated to ALEXA546. CaML1 protein appears red (K) and is localized to SymS (white arrows). Bacteroid nucleic acids in K stained with SYTO13 appear green (L). Overlay of K and L resulted in M. CaML1 protein surrounds the bacteroid nuclear material (scale bar = 3 μm for K and M). Light scattering from the fluorochrome can contribute to the SymS appearing broader than expected.

in association with the inner leaflet of the Sym membrane. Our demonstration that nodule-specific CaML1 protein, which has a presequence 75% identical to nodulin-25 and is found in the SymS, coupled with the fact that all *M. truncatula CAML* presequences are very similar (see Supplemental Fig. 1), argues that all are targeted to the SymS.

Fedorova et al. (2002) previously reported that optimal alignment of CaML proteins with the typical CaM proteins produced a gap occurring in domain II. Realignment of the CaML protein sequence without omitting the typical CaM protein sequence showed an additional complete functional EF hand in CaML1, 2, and 5 (see Supplemental Fig. 2).

Because *M. truncatula* nodule-specific CaMLs are atypical and have a variable number of EF hands, we thought it important to show that they do, in fact, bind Ca^{2+}. Typical CaMs have previously been shown to display a mobility shift when Ca^{2+} is bound (Lee et al., 1995; Camas et al., 2002; Zielinski, 2002). Utilizing recombinant His-CaML1 (three EF hands), a truncated His-CaML1 protein (EF-hands 3 and 4), a His-CaML4 protein (two EF hands), and a His-CaML6 protein (two EF hands), we performed Ca^{2+}-dependent mobility shift and ^{45}Ca-binding assays with the nodule-specific CaMLs. Both the His-CaML1 and the truncated His-CaML protein showed a Ca^{2+}-dependent mobility shift (Fig. 3B). However, no shift was observed for His-CaML4 or 6 (data not shown). As expected, the bovine CaM with bound Ca^{2+} showed increased mobility as compared to the Ca^{2+}-free protein. When recombinant CaML proteins and bovine CaM were incubated with ^{45}Ca in solution on protein blots, both G10- and His-CaML1 fusion proteins bound Ca^{2+} efficiently (Fig. 3C). The other His-tagged CaML proteins displayed a weaker binding of the labeled Ca^{2+} (data not shown). Our data indicate that all of the CaML proteins tested bind Ca^{2+}, but to varying degrees. This result was not unexpected because some of the EF hands do not conform to the canonical EF-hand motifs.

In efforts to define a function for nodule CaMLs, we have attempted RNAi-induced gene silencing. Results, however, have been inconsistent with phenotypes ranging from impaired symbiotic-dependent growth to no detectable effect (data not shown). We have tried silencing with constructs designed from CaML1, 4, and 6, but none have resulted in silencing of all six CaML messages. The lack of any of the constructs silencing the entire gene family along with the inconsistent phenotypes suggests that the individual CaMLs may not be functionally redundant.

Inclusively, our data provide evidence for a novel family of Ca^{2+}-binding proteins encoded by plant nuclear genes being incorporated into the SymS. Whereas the specific role of nodule-specific CaML proteins in symbiotic N_2 fixation remains to be established, it has become apparent that Ca^{2+} and Ca^{2+}-signaling events are involved in legume root nodule symbiosis from initial recognition events to endocytosis and cation channel gating in the Sym membrane. Substantial Ca^{2+} has been detected in the SymS, and Ca^{2+} within the SymS has been implicated in modulating the transport of fixed NH_4^+ (Andreeva et al., 1999; Roberts and Tyerman, 2002). However, it is thought that the free Ca^{2+} within Syms is low, with most being bound. Our data show that plant nodule-specific nuclear-encoded CaML proteins are found in the SymS of *M. truncatula* nodules and may be important in Ca^{2+} signaling. Ca^{2+} concentrations within the SymS may be regulated through oscillations in binding to CaML proteins. Moreover, nodule CaML conformation may be altered by Ca^{2+} binding, as occurs with typical CaMs, thereby regulating CaML interaction with other proteins in the SymS and/or Sym membrane. Binding and release of Ca^{2+} in the SymS would provide a rapid and efficient mechanism for regulating Ca^{2+} availability within the SymS and near the Sym membrane. CaMs and Ca^{2+} are known to affect endocytosis (Colombo et al., 1997), organelle-cytosol signaling (Yang and Poovaiah, 2003), Glu metabolism and the γ-aminobutyrate shunt (Bouché and Fromm, 2004), anion channel gating (Roberts and Tyerman, 2002), and adaptation to anaerobiosis (Rawsthorne and LaRue, 1986; Subbaiah and Sachs, 2003), processes also known to be intimately related to root nodule function. Whether nodule-specific CaMLs are involved in regulating these processes in *M. truncatula* remains to be established.

Co-Opting of *CaM* Genes for Sym Function

*CaML*s have distinct hybridization patterns in genomic blots and do not cross hybridize with *CaM*s under high stringency conditions (data not shown). Genomic library screening with a *CaML1* cDNA yielded one positive clone carrying two *CaML* genes in head-to-tail orientation separated by approximately 2.5 kb (GenBank AY542873). Sequence comparison with nodule-specific tentative consensus sequences (TIGR MtGI) indicated that these two genes, designated *CaML1* and *CaML2*, encoded CaML1 and CaML2 proteins, respectively. *CaML2* is upstream of *CaML1* and 160 bp of the intergenic region showed 85% identity with the 3′-untranslated region of the typical *M. truncatula CaM2*. Both *CaML1* and *CaML2* contained only one intron at identical positions, interrupting the presequence and CaM-like coding regions. In addition to the high sequence identity (88%) between the coding regions, the 770-bp intron sequence in *CaML1* and the 873-bp intron sequence in *CaML2* were 90% identical. Furthermore, the 0.5 kb upstream of the ATG start codon were 99% identical. Analysis of the presumptive *CaML1* and *CaML2* promoter sequences revealed that four copies of a putative cis-element (CTCTT) were present within 1 kb of the *CaML1* translation start site. CTCTT is known to be one of the critical cis-elements in nodulin gene promoters and thus may also contribute to the high-level *CaML1* gene expression in nodules (Sandal et al., 1987).

We identified additional genomic regions corresponding to *CaML* and typical *CaM* (*CaM1* and *CaM2*)

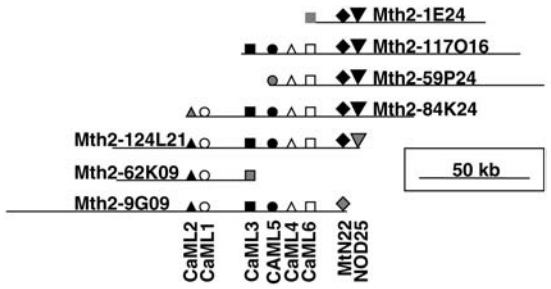

Figure 4. All six *M. truncatula CaML* genes, *nodulin-25*, and *nodulin-22* cluster within 112 kb of the *M. truncatula* genome. BLASTN analysis identified BAC-end sequence matches (shaded gray) to *CaML2*, *CaML3*, *CaML5*, *CaML6*, *nodulin-22*, and *nodulin-25*. PCR amplification was performed on all seven BACs using primers designed from *CaML1* (○), *CaML2* (▲), *CaML3* (■), *CaML4* (△), *CaML5* (●), *CaML6* (□), *nodulin-25* (◇), and *nodulin-22* (▼). The results of PCR amplification were used to order the genes on the contig. For final verification, PCR products from the amplification of all eight genes using BAC Mth2-124L21 as template were cloned and sequenced.

genes by using their nucleotide sequences as BLASTN queries (Altschul et al., 1997) against the available *M. truncatula* genome sequence (November, 2005). We found exact bacterial artificial chromosome (BAC)-end matches for portions of *CaML2*, *3*, *5*, and *6* (Fig. 3). Comparisons of cDNA and BAC-end sequences identified portions of intron sequences in *CaML3*, *5*, and *6*. *CaML3*, *5*, and *6* also contained a single intron of varying size in the presequence.

The *CaM* and *CaML* sequences matching BAC identifiers were used to query the fingerprinted BAC contigs at the *M. truncatula* genome Web site (http://mtgenome.ucdavis.edu). The BACs corresponding to *CaM1* and *CaM2* were in separate contigs (contigs 230 and 1,307, respectively), whereas the BACs corresponding to *CaML2*, *3*, and *6* all belonged to contig 410. The fact that *CaML1* and *CaML2* occur in close proximity indicates that at least four *CaML* sequences were clustered within contig 410 (420 kb). *CaML5* was located on a singleton BAC (Mth2-59P24). PCR amplification from a subset of BAC clones containing the identified *CaML* BAC ends using gene-specific *CaML* primers not only placed the singleton BAC containing *CaML5* in contig 410, but also placed the final known member of the *CaML* gene family, *CaML4*, in the contig (Fig. 4; GenBank AY542873, AY649559–AY649562).

Analysis of available BAC-end sequence data from contig 410 also revealed exact matches to nodulin-22 (GenBank CAA75576) and nodulin-25 protein (GenBank CAB91091; see supplemental data for additional matches). Alignment of BAC-end sequences from Mth2-1D09 and Mth2-124L21 with the complete *nodulin-25* gene (GenBank AJ277858) revealed 100% nucleotide identity, largely to intron sequence. Primers designed from *nodulin-22* and *nodulin-25* and PCR analysis confirmed the positions of these genes in the contig (Fig. 4). As a final verification of our results, specific primers corresponding to *CaML1* to *6*, *nodulin-25*, and *nodulin-22* were used for PCR amplification of these sequences from BAC Mth2-124L21, which was predicted to contain all eight genes. The PCR products were cloned and subsequent sequencing matched the sequences of the eight genes and confirmed the location of these genes. Based on the size of this BAC (D. Cook, personal communication), all six *CaML* genes, *nodulin-25*, and *nodulin-22* clustered within a 112-kb region.

Given the proximity of *nodulin-25* to the *CaML* genes and the amino acid similarity shared among their presequences, the entire *nodulin-25* gene and available promoter sequence was compared to the *CaML1* and *CaML2* genomic sequences (see Supplemental Fig. 2). *Nodulin-25* shared 75% nucleotide similarity over 363 bases with *CaML1* and *CaML2*. The first 221 bases of identity corresponded to putative promoter regions. Similarity extended through exon 1 (103 bp) and continued through the first 40 bp of intron 1. These results suggest an unequal recombination event between *nodulin-25*, and a nearby *CaM* fused a portion of the *nodulin-25* to the *CaM*, which created a nodule-specific *CaML* gene. Evolution of the *CaML*s through an unequal recombination event involving *nodulin-25* is not surprising. Végh et al. (1990) proposed that *nodulin-25* evolved primarily through exon shuffling. Of the 13 nodulin-25 exons, 10 are the same size (54 bp)

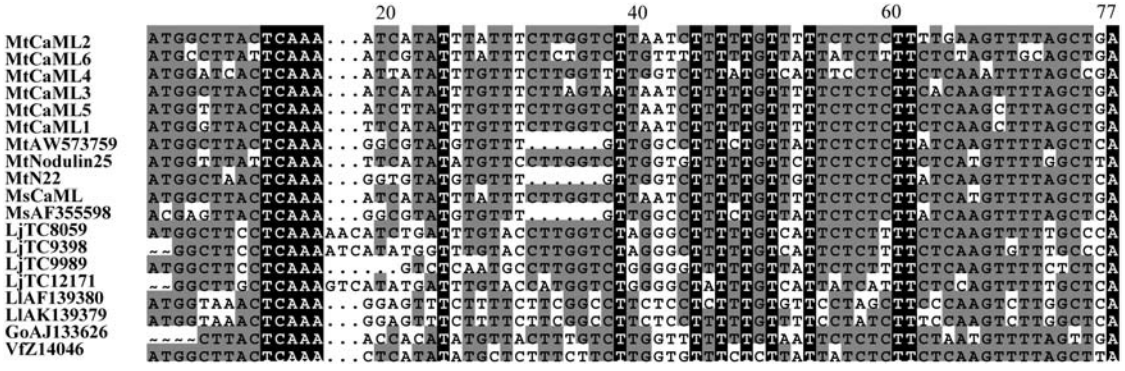

Figure 5. Multiple sequence alignment of conserved nodule-specific signal peptides in eight unique genes or gene families. Designations at left are GenBank accession numbers, TIGR tentative consensus identifiers, or MsCaM and MtCaML numbers.

and show up to 94% sequence similarity with each other. Misalignment anywhere in the *nodulin-25* gene could have resulted in an unequal recombination event between *nodulin-25* and a nearby *CaM*.

To determine the relationship between *CaM* and *CaML* genes, we constructed a phylogenetic tree from the coding sequences of 112 full-length *CaM*s and *CaML*s representing 40 different species within the Viridiplantae (see Supplemental Figs. 3 and 4). As controls, we included the sequences of two typical *CaM*s from *M. truncatula* (*CaM1* and *CaM2*). Given their proximity in the genome, it is not surprising that we found all six *M. truncatula CaML* sequences clustered into a single separate clade in 75 of 100 bootstrap replicates. Significant support (bootstrap score of 100) was found for the separation of *M. truncatula CaML*s *1* to *4*. Lower support for *M. truncatula CaML5* and *CaML6* may be due to internal deletions that would reduce the number of informative sites used in phylogenetic analysis. It is noteworthy that *M. truncatula CaM2* and a *CaM* from alfalfa were also distinct from the typical *CaM*s (bootstrap score of 97). The observation that 160 bp of the intergenic region between *CaML1* and *CaML2* was similar to the 3′-untranslated region of *CaM2* supports our observation that the *CaML* genes descended from *CaM2*. The separation of *M. truncatula CaML* sequences into a different clade from typical *CaM*s indicates they have diverged significantly.

Our phylogenetic analysis indicates that all six *CaML*s likely arose from a single *CaML* progenitor. The step-like pattern observed in the *M. truncatula CaML* clade suggests that these genes evolved by tandem duplication and divergence. Sequencing the genome fragment corresponding to *CaML1* and *CaML2* revealed they were the result of a duplication event. Additional duplication events likely gave rise to other *CaML* genes within this cluster. Once the *CaML* gene cluster expanded, its members could also undergo unequal recombination. Not only are multiple *CaML*s present, but each of these genes is made up of repetitive EF hands. Mispairing between *CaML* genes followed by recombination allows expansion or contraction of *CaML* gene copy number to occur. Mispairing of EF hands within a *CaML* followed by recombination would allow changes in the number of EF hands within a gene and shuffling of EF hands. The variation in numbers of EF hands between *CaML*s provides overwhelming evidence that this has occurred. Further sequence analysis of contig 410 could provide additional evidence of duplication and may allow identification of the progenitor gene.

We have recently found at least one *CaML* gene expressed in alfalfa and *Lotus japonicus* (S. Miller and M. Graham, unpublished data; TIGR LjGI at www.tigr.org/tdb/tgi/plant.shtml, TC8059, respectively), providing evidence for their existence in other legume species. Identification of additional CaMLs awaits further sequencing of legume genomes. In addition, using a motif model based on the presequence of *M. truncatula nodulin-22*, *nodulin-25*, and the *CaMLs*, we have been able to identify eight unique genes or gene families containing a highly similar presequence. These sequences were identified from the following species either as cloned cDNAs or EST sequences: Lotus, alfalfa, *Lupinus luteus*, *Galega orientalis*, and *V. faba* (Fig. 5). For several sequences, multiple splice products were detected. Alternate splice products were not detected within the signal peptide; therefore, redundant sequences were not included. Consistent with our finding with the *M. truncatula CaMLs*, all sequences were isolated from root nodule libraries.

CONCLUSION

In this article, we provide biochemical and genomic evidence for a plant gene being co-opted and recruited for root nodule symbiosis. We have demonstrated that nodule *CaMLs* diverged from a progenitor gene to create a distinct set of Ca^{2+}-binding proteins. These Ca^{2+}-binding proteins are nodule specific, expressed uniformly at 6 DAI, and located in the SymS. Moreover, nodule CaMLs are clustered in the genome of *M. truncatula* along with at least two other nodule-specific genes. Whereas we have not defined the specific function of nodule-specific CaMLs, based upon their location in the SymS and the fact that Ca^{2+} flux affects anion channel gating, they appear to be integrally related to Sym function.

Szczyglowski and Amyot (2003) and others (Albrecht et al., 1999) have previously discussed other examples that might exemplify recruitment of symbiotic function genes from existing plant programs. The origins of *ENOD* genes, the genetic determinants underlying the arbuscular mycorrhizal and Rhizobium symbioses, and genes involved in autoregulation of nodulation all appear to have been borrowed from preexisting developmental and signaling pathways. In addition, the O_2-carrying heme protein leghemoglobin, unique to nodules, is likely a specialized product of divergence from ancestral plant hemoglobins that may have been derived from a hemoglobin gene in the last common ancestor to plants and animals (Hardison, 1996). The genomic arrangement and phylogeny of *M. truncatula CaML*s, coupled with the localization of CaML protein in the SymS, conclusively demonstrate gene recruitment for symbiotic purposes. The fact that CaML proteins are located in the SymS and that they can bind Ca^{2+} make them likely candidates for mediating signal transduction and/or communication between the host plant and microbial symbiont.

MATERIALS AND METHODS

Plant Materials, Bacterial Strains, and Protein Standards

Medicago truncatula (Gaertn.) seeds, line A17 of cv Jemalong, were acid scarified and planted in a glasshouse as previously described (Fedorova et al., 2002). For the RT-PCR experiment, plants were inoculated with *Sinorhizobium meliloti* strain 102F51 11 days following planting. *M. truncatula* seeds were inoculated at planting with ineffective *S. meliloti* strain T202 (oxygen regulation mutant; Virts et al., 1988) and the nodules were harvested 12 DAI for RNA

extraction or 19 and 31 DAI for in situ hybridization. For protein blotting and RNA extraction, seeds were inoculated with *S. meliloti* 102F51 at planting and nodules were harvested 8, 10, and 14 d later. All tissues were harvested into liquid nitrogen except those tissues used for in situ hybridizations, which were placed directly in fixative. Bovine brain CaM was obtained from Sigma.

PCR Primer Sequences

The sequence of primers used to construct fusion proteins can be found in Supplemental Table I. Primer sequences for RT-PCR reactions and the *CaML* genes from BAC clones can be found in Supplemental Table II. Specificity of the CaML primers was demonstrated as described below. Primer pairs for CaML4, 5, and 6 spanned introns of unequal sizes; therefore, the approximately 800-, 1,000-, and 400-bp products generated, respectively, were easily distinguished as unique to those genes. The single introns in CaML1, 2, and 3 are highly homologous. The primer pairs for CaML2 and CaML3 shared a forward primer designed to anneal to DNA in an area of their introns for which a gap existed in the CaML1 intron and therefore would not allow amplification of CaML1. Annealing temperature gradients were run on positive and negative control DNAs and it was determined that the CaML2 primer pair PCR run with a 67.5°C annealing temperature distinguished CaML2 from CaML3 and, likewise, the CaML primer pair PCR run with an annealing temperature of 65°C distinguished CaML3 from CaML2. The primer pair designed to PCR CaML1 had 3- to 6-bp mismatches or missing bases in both the 3′- and 5′-priming sites as compared to both CaML2 and CaML3 DNA; therefore, no products for CaML2 or CaML3 were observed at an annealing temperature of 55°C. Additionally, to demonstrate specificity, CaML2 to 6 PCR products were directly sequenced from those reactions following cleanup using a QIAquick PCR purification kit (Qiagen) and found to be pure products.

RNAi and Plant Transformation

Fragments of the 5′ ends of three *CaML* genes were amplified by PCR from cDNA clones EST482240 (TC86088, CaML1, 165 bp), EST483481 (TC88152, CaML6, 255 bp), and EST484686 (TC79618, CaML4, 238 bp) and the products were introduced into RNAi-inducing pHellsgate 8 vector (Helliwell et al., 2002) using the GATEWAY system (Invitrogen), creating pHG8:1277i, pHG8:1278i, and pHG8:1279i, respectively. The pHellsgate 8 vector with a fragment of the GUS or lacZ gene was used as a control. Proper insertion of the PCR products into the vector was verified by sequencing. *M. truncatula* (A17) seedling radicles were transformed using *Agrobacterium rhizogenes* ARqual to generate hairy roots with the recombinant vectors as described (Boisson-Dernier et al., 2001; Ivashuta et al., 2005).

Production of Fusion Protein and Antiserum

The pGEMEX T7 (Promega) and Qiaexpress pQE30 (Qiagen) vector systems were used to produce recombinant CaML1 proteins, designated G10-CaML1 and His-CaML1 proteins, respectively, for use in antibody production and IgG affinity purification. Rabbit polyclonal antiserum was produced against the gel-purified G10-CaML1 protein as described elsewhere (Vance et al., 1985).

MS

The identity of the electroeluted G10-CaML protein was confirmed by matrix-assisted laser-desorption ionization time-of-flight MS (Biemann, 1992) using a Bruker Biflex III instrument with a nitrogen laser for ionization (University of Minnesota spectrometry facility). The EXPASy peptide mass program (http://ca.expasy.org) was used to predict the M_r of the expected tryptic digest fragments.

Acetone-precipitated SymS proteins (40 μg) were separated on a 12.5% SDS-PAGE gel and stained with Coomassie Brilliant Blue. A protein band corresponding to a CaML1 antibody-reactive band from immunoblot analysis of this fraction was excised and an in-gel tryptic digest was performed (as detailed at www.cbs.umn.edu/mass_spec/ingel3.htm). Two peaks from the matrix-assisted laser-desorption ionization-MS run, tentatively identified as possible CaML protein fragments, were subjected to tandem MS (Biemann, 1992) on an ABI QSTAR XL. The data obtained were used to search the National Center for Biotechnology Information nonredundant database using the peptide mass fingerprint option in the Mascot search program (www.matrixscience.com).

Protein Electrophoresis and Immunoblotting

Total proteins from various tissues of *M. truncatula* were ground in 1 × SDS gel sample buffer, boiled, and centrifuged, then separated by 12.5% SDS-PAGE and transferred to nitrocellulose (Miller et al., 2001). *M. truncatula* SymS proteins were isolated from nodules 14 DAI using differential centrifugation as detailed by Catalano et al. (2004).

Mobility shift assays were carried out by combining aliquots of bovine CaM or the purified 6 × His-CaML proteins with either $CaCl_2$ or EGTA (to 1 mM final concentrations) as previously described (Camas et al., 2002). The immunoblot was incubated with a mixture of eluted CaML1 protein antibodies and antibodies that recognize bovine CaM (Zymed). Bound antibodies were visualized using the ECL western-blotting detection system (Amersham Biosciences).

In Vitro ^{45}Ca-Binding and Mobility Shift Experiments

Purified proteins were separated by 4% to 12% gradient SDS-PAGE (Invitrogen), transferred to nitrocellulose, and ^{45}Ca binding determined as described by Maruyama et al. (1984).

Construction and Screening of the *M. truncatula* Genomic Library

Genomic DNA isolated from young leaves of *M. truncatula* plants was digested with *Bam*HI, fractionated, and cloned into the λDASH II (*Bam*HI) vector (Stratagene) as previously described (Miller et al., 2001). A cDNA insert representing the nodule-specific CaML1 protein was labeled and hybridized to plaque lifts in 7% SDS, 0.5 M $Na_2H_2PO_4$ at 68°C. A hybridizing clone with an 18-kb insert was identified and subcloned into pBS(SK) (Stratagene) for restriction mapping and sequencing.

Construction and Analysis of Chimeric Reporter Genes

A 1.6-kb sequence upstream of the ATG start codon was amplified by PCR from the genomic clone *CaML1* and inserted into pBI101.2 (CLONTECH) containing either the GUS or GFP reporter gene for plant transformation. The recombinant plasmids were introduced separately into *Agrobacterium tumefaciens* strain LBA4404 by electroporation. Alfalfa (*Medicago sativa*) transformations were carried out as essentially described by Austin et al. (1995). Transformed cells were regenerated and plants propagated as vegetative cuttings.

In Situ Hybridization, Immunocytochemical, and Immunogold Localization

In situ hybridization and probe preparation were carried out according to the methods described by Trepp et al. (1999). The probes used were linearized from pBS(SK) plasmids containing an 800-bp (*Xho*I-*Not*I) *CaML1* cDNA fragment, a 900-bp *M. truncatula CaM1* fragment, or a 700-bp leghemoglobin fragment (a gift from Ann Hirsch, University of California, Los Angeles).

Fifteen DAI *M. truncatula* nodules were hand sectioned and immunolabeled according to a modified version of Harrison et al. (2002). Nodule sections were fixed for 2 h in 4% formaldehyde and 5% dimethyl sulfoxide (v/v) in PME buffer (50 mM PIPES, 5 mM $MgSO_4$, and 10 mM EGTA, pH 7.0). Nodule sections were rinsed three times for 10 min with PME and then digested in 1% Cellulase-RS, 0.01% pectolyase Y23 (Karlan Research Products), and 1% bovine serum albumin in PME buffer for 1 h. Nodule sections were rinsed three times for 5 min with PME and then incubated for 1 h in 3% bovine serum albumin, 1% normal goat serum in Tris-buffered saline (TBS), pH 7.4. The blocking solution was removed and the nodule sections were incubated in purified anti-CaML1 antibody at 1:5 in block. Nodule sections were then rinsed three times for 10 min in TBS and incubated in a 1:20 dilution of goat anti-rabbit IgG ALEXA546 secondary antibody (Molecular Probes) and a dilution of 1:1,000 SYTO13 (Molecular Probes) nucleic acid stain for 1 h. Nodule sections were rinsed three times for 10 min with TBS and images were acquired on an inverted Zeiss LSM 510 NLO laser-scanning microscope (Carl Zeiss).

Immunogold labeling was carried out according to Robinson et al. (1994).

Identification of Genome Sequence Corresponding to CaM and CaML

BLASTN analysis (Altschul et al., 1997) of *M. truncatula CaML1* to *6*, *M. truncatula CaM1* (GenBank AF494219), and *M. truncatula CaM2* (GenBank AF494220) against the available *M. truncatula* genome sequence was used to identify matching BACs. To determine whether identified BACs were present in the same contig, BAC names were used to query the *M. truncatula* genome Web site at the University of California, Davis (http://mtgenome.ucdavis.edu). BAC-end sequences from other BACs present in contig 410 were compared to the GenBank nonredundant database (April, 2004; BLASTX) to identify additional genes of interest. Gene-specific primers designed for *nodulin-25* and *nodulin-22* were used to position the genes in the contig.

Analysis of Medicago BAC Contig 410

To determine sequences of interest in contig 410, all available BAC-end sequences from the contig were compared to the GenBank nonredundant database using BLASTX (April, 2004). Identified sequence matches included MtN22 (GenBank Y15294) and nodulin-25 (GenBank AJ277858). PCR amplification with gene-specific primers was used to verify the assembly of contig 410 to determine whether BAC Mth2-59P24 belonged to the contig and to position all six *CaML* genes, *nodulin-25*, and *nodulin-22* in the contig. As final validation, gene-specific primers from the six *CaML* genes, *nodulin-25*, and *nodulin-22* were used in amplification reactions using the core BAC Mth2-124L21 as template. The PCR products were cloned and sequenced to verify the presence of all eight genes. See Supplemental Table II for all primers used in BAC PCR procedures.

Phylogenetic Analyses of CaM and CaML Sequences

The *M. truncatula* CaML1-6 sequences (containing the presequence) were blasted against the following databases to determine whether homologs were present in other species: GenBank nonredundant (BLASTX) and dBEST (tBLASTX), TIGR (*Oryza sativa*; March, 2004) and Arabidopsis (*Arabidopsis thaliana*; version 4) genome databases. No homologs containing a similar presequence were identified; therefore, alignments were made with all six CAML coding sequences and 106 additional Viridiplantae CaM sequences identified from GenBank. Prior to phylogenetic analysis, the presequence was removed from the six CAML sequences. Phylogenetic trees of the alignment were constructed using the Genetics Computer Group programs PAUPSEARCH and PAUPDISPLAY.

Disclaimer

Mention of trade names or commercial products in the article is solely for the purpose of providing specific information and does not imply recommendations or endorsement by the U.S. Department of Agriculture.

Note Added in Proof

Following submission of this article, the sequence of BAC 124L21 (CT573353) was released by the *Medicago truncatula* Genome Sequencing Consortium. Currently, the sequence has been assembled into four contigs totaling 148,036 bases. Detailed analyses will be performed following completion of sequencing. However, the available sequence confirms the presence of *nodulin-25*, *nodulin-22*, and *CaML1* through *6* on BAC 124L21. In addition, all eight genes share between 163 and 1,353 bases of promoter sequence and between 128 and 138 bases of sequence corresponding to the signal peptide. These results support the conclusions drawn in this article.

Sequence data from this article for the DNA and protein sequences can be found in the GenBank/EMBL data libraries under accession numbers AY542873 (*M. truncatula CAML1* and *CAML2*), AY649559 to AY649562 (partial BAC sequences for *CAML3–6*), AY649556 (*nodulin-22*), and AY649555 (*nodulin-25*).

ACKNOWLEDGMENTS

We thank Kirk Czymmek for assistance with microscopic analysis in the immunocytochemical localization carried out at the Delaware Biotechnology Institute by C.M. Catalano. We also thank Mindy Dornbusch for generation of the transformed alfalfa plants. SymS protein was provided by D.J. Sherrier and C.M. Catalano. Special thanks to Dr. Mark Sanders for his direction of B. Bucciarelli with the use of the confocal microscope and his assistance in image processing.

Received January 12, 2006; revised January 12, 2006; accepted February 16, 2006; published March 16, 2006.

LITERATURE CITED

Albrecht C, Geurts R, Bisseling T (1999) Legume nodulations and mycorrhizae formation; two extremes in host specificity meet. EMBO J **18:** 281–288

Altschul SF, Madden TL, Schaffer AA, Zhang J, Zhang Z, Miller W, Lipman D (1997) Gapped BLAST and PSI-BLAST: a new generation of protein database search programs. Nucleic Acids Res **25:** 3389–3402

Andreeva IN, Andreev IM, Dubrovo PN, Kozharinova GM, Krylova VV, Izmailov SF (1999) Calcium stores in symbiosomes from yellow lupin root nodules. J Plant Physiol **155:** 357–363

Austin S, Bingham ET, Mathews DE, Shahan MN, Will J, Burgess RR (1995) Production and field performance of transgenic alfalfa (*Medicago sativa* L.) expressing alpha-amylase and manganese-dependent lignin peroxidase. Euphytica **85:** 381–393

Biemann K (1992) Mass spectrometry of peptides and proteins. Annu Rev Biochem **61:** 977–1010

Boisson-Dernier A, Chabaud M, Garcia F, Becard G, Rosenberg C, Barker DG (2001) *Agrobacterium rhizogenes*-transformed roots of *Medicago truncatula* for the study of nitrogen-fixing and endomycorrhizal symbiotic associations. Mol Plant Microbe Interact **14:** 695–700

Bouché N, Fromm H (2004) GABA in plants: just a metabolite? Trends Plant Sci **3:** 110–115

Camas A, Cardenas L, Quinto C, Lara M (2002) Expression of different calmodulin genes in bean (*Phaseolus vulgaris* L.): role of nod factor on calmodulin gene regulation. Mol Plant Microbe Interact **15:** 428–436

Catalano CM, Lane WS, Sherrier DJ (2004) Biochemical characterization of symbiosome membrane proteins from *Medicago truncatula* root nodules. Electrophoresis **25:** 519–531

Colombo MI, Beron W, Stahl PD (1997) Calmodulin regulates endosome fusion. J Biol Chem **272:** 7707–7712

Dahiya P, Kardailsky IV, Brewin NJ (1997) Immunolocalization of PsNLEC-1, a lectin-like glycoprotein expressed in developing pea nodules. Plant Physiol **115:** 1431–1442

Fedorova M, van de Mortel J, Matsumoto PA, Cho J, Town CD, VandenBosch KA, Gantt JS, Vance CP (2002) Genome-wide identification of nodule-specific transcripts in the model legume *Medicago truncatula*. Plant Physiol **130:** 519–537

Geurts R, Bisseling T (2002) Rhizobium nod factor perception and signalling. Plant Cell (Suppl) **14:** S239–S249

Graham P, Vance CP (2003) Legumes: importance and constraints to greater use. Plant Physiol **131:** 872–877

Hardison RC (1996) A brief history of hemoglobins: plant, animal, protist, and bacteria. Proc Natl Acad Sci USA **93:** 5675–5679

Harrison MJ, Dewbre GR, Liu J (2002) A phosphate transporter from *Medicago truncatula* involved in the acquistion of phosphate released by arbuscular mycorrhizal fungi. Plant Cell **14:** 2413–2430

Helliwell CA, Wesley SV, Wielppolska AJ, Waterhouse PM (2002) High-throughput vectors for efficient gene silencing in plants. Funct Plant Biol **29:** 1217–1225

Ivashuta S, Liu J, Liu J, Lohar DP, Haridas S, Bucciarelli B, VandenBosch KA, Vance CP, Harrison MJ, Gantt JS (2005) RNA interference identifies a calcium-dependent protein kinase involved in *Medicago truncatula* root development. Plant Cell **17:** 2911–2921

Kiss GB, Vincze E, Végh Z, Toth G, Soos J (1990) Identification and cDNA cloning of a new nodule-specific gene, Nms-25 (nodulin-25) of *Medicago sativa*. Plant Mol Biol **14:** 467–475

Krylova VV, Andreev IM, Andreeva IN, Dubrovo PN, Kozharinova GM, Izmailov SF (2002) Verapamil-sensitive calcium transporter in the

peribacteroid membrane of symbiosomes from *Vicia faba* root nodules. Russ J Plant Physiol **49:** 746–753

Lee SH, Kim JC, Lee MS, Heo WD, Seo HY, Yoon HW, Hong JC, Lee SY, Bahk JD, Hwang I, et al (1995) Identification of a novel divergent calmodulin isoform from soybean which has differential ability to activate calmodulin-dependent enzymes. J Biol Chem **270:** 21806–21812

Lévy J, Bres C, Geurts R, Chalhoub B, Kulikova O, Duc G, Journet E-P, Ané J-M, Lauber E, Bisseling T, et al (2004) A putative Ca^{2+} and calmodulin-dependent protein kinase required for bacterial and fungal symbioses. Science **303:** 1361–1364

Maruyama K, Mikawa T, Ebashi S (1984) Detection of calcium binding proteins by ^{45}Ca autoradiography on nitrocellulose membrane after sodium dodecyl sulfate gel electrophoresis. J Biochem (Tokyo) **95:** 511–519

Mellor RB, Werner D (1987) Peribacteroid membrane biogenesis in mature legume root nodules. Symbiosis **3:** 75–100

Miller SS, Liu J, Allan DL, Menzhuber CJ, Fedorova M, Vance CP (2001) Molecular control of acid phosphatase secretion into the rhizosphere of proteoid roots from phosphorus-stressed white lupin. Plant Physiol **127:** 594–606

Mitra RM, Gleason CA, Edwards A, Hadfield J, Downie JA, Oldroyd GED, Long SR (2004) A Ca^{2+}/calmodulin-dependent protein kinase required for symbiotic nodule development: gene identification by transcript-based cloning. Proc Natl Acad Sci USA **101:** 4701–4705

Mitra RM, Long SR (2004) Plant and bacterial symbiotic mutants define three transcriptionally distinct stages in the development of the *Medicago truncatula*/*Sinorhizobium meliloti* symbiosis. Plant Physiol **134:** 595–604

Mylona P, Pawlowski K, Bisseling T (1995) Symbiotic nitrogen fixation. Plant Cell **7:** 869–885

Panter S, Thomson R, deBruxelles G, Laver D, Trevaskis B, Udvardi M (2000) Identification with proteomics of novel proteins associated with the peribacteroid membrane of soybean root nodules. Mol Plant Microbe Interact **3:** 325–333

Rawsthorne S, LaRue TA (1986) Metabolism under microaerobic conditions of mitochondria from cowpea nodules. Plant Physiol **81:** 1097–1102

Reddy ASN (2001) Calcium: silver bullet in signaling. Plant Sci **160:** 381–404

Roberts DM, Tyerman SD (2002) Voltage-dependent cation channels permeable to NH_4^+, K^+, and Ca^{2+} in the symbiosome membrane of the model legume *Lotus japonicus*. Plant Physiol **128:** 370–378

Robinson DL, Kahn ML, Vance CP (1994) Cellular localization of nodule-enhanced aspartate aminotransferase in *Medicago sativa* L. Planta **192:** 202–210

Saalbach G, Erik P, Wienkoop S (2002) Characterization by proteomics of peribacteroid space and peribacteroid membrane preparations from pea (*Pisum sativum*) symbiosomes. Proteomics **2:** 325–327

Sandal NN, Bojsen K, Marcker KA (1987) A small family of nodule specific genes from soybean. Nucleic Acids Res **15:** 1507–1519

Sanders D, Brownlee C, Harper JF (1999) Communicating with calcium. Plant Cell **11:** 691–706

Shaw SL, Long SR (2003) Nod factor elicits two separable calcium responses in *Medicago truncatula* root hair cells. Plant Physiol **131:** 976–984

Simonsen AC, Rosendahl L (2002) Origin of de novo synthesized proteins in different compartments of pea-*Rhizobium* sp. symbiosomes. Mol Plant Microbe Interact **12:** 319–327

Snedden WA, Fromm H (2001) Calmodulin, a versatile calcium signal transducer in plants. New Phytol **151:** 35–66

Son O, Yang H-S, Lee H-J, Lee M-Y, Shin K-H, Jeon S-L, Lee M-S, Choi S-Y, Chun J-Y, Kim H, et al (2003) Expression of *srab7* and *ScaM* genes required for endocytosis of *Rhizobium* in root nodules. Plant Sci **165:** 1239–1244

Subbaiah CC, Sachs MM (2003) Molecular and cellular adaptions of maize to flooding stress. Ann Bot (Lond) **90:** 119–127

Szczyglowski K, Amyot L (2003) Symbiosis, inventiveness by recruitment. Plant Physiol **131:** 935–940

Trepp GB, Temple SJ, Bucciarelli B, Shi L, Vance CP (1999) Expression map for genes involved in nitrogen and carbon metabolism in alfalfa root nodules. Mol Plant Microbe Interact **12:** 526–535

Udvardi MK, Day DA (1997) Metabolite transport across symbiotic membranes of legume nodules. Annu Rev Plant Physiol Plant Mol Biol **48:** 493–523

Vance CP (2002) Root-bacteria interactions: symbiotic N_2 fixation. *In* Y Waisel, A Eshel, U Kafkafi, eds, Plant Roots: The Hidden Half. Marcel Dekker, Inc, New York, pp 839–867

Vance CP, Boylan KLM, Stade S, Somers DA (1985) Nodule specific proteins in alfalfa (*Medicago sativa* L.). Symbiosis **1:** 69–84

Vasse J, de Billy F, Camut S, Truchet G (1990) Correlation between ultrastructure, differentiation of bacteroids and nitrogen fixation. J Bacteriol **172:** 4295–4306

Végh Z, Vincze É, Kadirov R, Tóth G, Kiss GB (1990) The nucleotide sequence of a nodule-specific gene Nms-25 of *Medicago sativa*: its primary evolution via exon-shuffling and retrotransposon-mediated DNA rearrangements. Plant Mol Biol **15:** 295–306

Vincent JL, Brewin NJ (2000) Immunolocalization of a cysteine protease in vacuoles, vesicles, and symbiosomes of pea nodule cells. Plant Physiol **123:** 521–530

Virts EL, Stanfield SW, Helinski DR (1988) Common regulatory elements control symbiotic and microaerobic induction of *nif A* in *Rhizobium meliloti*. Proc Natl Acad Sci USA **85:** 3062–3065

Webb KJ, Skot L, Nicholson MN, Jorgensen B, Mizen S (2000) *Mesorhizobium loti* increases root specific expression of a calcium-binding protein homologue identified by promoter tagging in *Lotus japonicus*. Mol Plant Microbe Interact **13:** 606–616

Weinkoop S, Saalbach G (2003) Proteome analysis: novel proteins identified at the peribacteroid membrane from *Lotus japonicus* root nodules. Plant Physiol **131:** 1080–1090

Werner PJ, Bassarab S, Humbeck C, Kape R, Kinnback A, Mellor RB, Mörschel E, Parniske M, Pausch G, Röhm M, et al (1988) Nodule proteins and compartments. *In* H Bothe, FJ de Bruijn, WE Newton, eds, Nitrogen Fixation: Hundred Years After. Gustav Fischer, New York, pp 507–515

White PJ (2000) Calcium channels in higher plants. Biochim Biophys Acta **1465:** 171–189

Yang T, Poovaiah BW (2003) Calcium/calmodulin-mediated signal network in plants. Trends Plant Sci **8:** 505–512

Zielinski RE (1998) Calmodulin and calmodulin-binding proteins in plants. Annu Rev Plant Physiol Plant Mol Biol **49:** 697–725

Zielinski RE (2002) Characterization of three new members of the *Arabidopsis thaliana* calmodulin gene family: conserved and highly diverged members of the gene family functionally complement a yeast calmodulin null. Planta **214:** 446–455